Mechanics of Advanced Composite Structures

Journal homepage: https://macs.semnan.ac.ir/

Semnan University

ISSN:2423-7043

Research Article

Investigation of the Mechanical and Tribological Behaviour of Al Alloy and Al/ZrO2Ex-Situ Nano Composites

Bhavana Singh [a]*, Vaibhav Trivedi [a], Ankur Goel [b]

[a] *Department of Mechanical Engineering, SET IFTM UNIVERSITY, Moradabad, 244001, India*

[b] *Orthopedic, Sri sai super specialityHospital, Moradabad, 244001, India*

ARTICLE INFO

Article history:

Received: 2025-03-20

Revised: 2025-12-06

Accepted: 2026-01-02

Keywords:

Al/ZrO_2 composites;

Mechanical properties;

Tribological behaviour;

Microstructure;

AFM;

Topography.

ABSTRACT

The present study investigates the mechanical and tribological behaviour of Al alloys and Al/ZrO_2 ex-situ composites, focusing on their microstructural evolution and property enhancement. Al/ZrO_2 composites were synthesised using stir casting, incorporating 1, 3, and 5 wt.% ZrO_2 particles. Alloys and composites were characterizedusing X-ray diffraction (XRD), optical microscope (OM), and scanning electron microscopy (SEM)to analyse phase formation, particle distribution. Microstructural analysis revealed homogeneous dispersion of ZrO_2 particles, promoting load transfer and matrix strengthening. Mechanical properties were analysed using Vickers microhardness and uniaxial tensile tests, demonstrating substantial increases in hardness and tensile strength with increasing ZrO_2 content due to grain refinement, dislocation strengthening, and Orowan strengthening mechanisms. Tribological performance was evaluated using a pin-on-disc apparatus under varying loads (10N- 30N) and sliding speeds (1 m/sec -3 m/sec). The Al/ZrO_2 composites exhibited a significant reduction in the wear (up to 50%) compared to the unreinforced alloy, attributed to the load-bearing capacity of ZrO_2 particles and the formation of a protective tribolayer. Surface morphology of the worn samples, analysed using SEM, indicated a transition from abrasive to mild adhesive wear with the addition of ZrO_2. Further topographical parameters were studied using atomic force microscopy (AFM), which suggests a decrease in surface roughness from 0.87 µm to 0.70 µm at3wt. % of ZrO_2 compared to the base alloy.

1. Introduction

Tribology is the study of friction, wear, and lubrication. Tribology is the key factor in the performance and longevity of moving components. Components subjected to repeated sliding or rolling contact often face severe wear and heat dissipation owing to friction [1-3]. The selection of materials with optimized tribological characteristics is important to minimize wear and enhance the efficiency of mechanical components. To fulfil these needs, developing materials with superior mechanical and tribological properties has become an important area of research to meet the rising need for high-performance engineering uses [4-5].

Aluminium (Al) alloys have gained widespread popularity in tribological applications because of their various attractive characteristics, such as low density, high specific strength, andthermal conductivity. These properties make Al-based alloys suitable for

* **Corresponding author.**

E-mail address: bhavnasingh15619@gmail.com

Cite this article as:

Singh, B., Trivedi, V. and Goel, A., 2027. I Investigation of the Mechanical and Tribological Behaviour of Al Alloy and Al/ZrO2Ex-Situ Nano Composites. *Mechanics of Advanced Composite Structures*, 14(1), pp. 19-26.

https://doi.org/10.22075/MACS.2026.37138.1824

components such as pistons, cylinder blocks, and brake rotors in the automobile and aerospace industries. However, because of theirrelatively lower hardness and wear resistance, conventional Al-based alloys restrict their effectiveness in tribological applications where high friction and wear are predominant [6-8].

To negate these restrictions, aluminium-based metal matrix composites (Al-MMCs) reinforced with ceramic particles have been developed. These composites acquire the required properties of Al alloys with the improved hardness and wear resistance of ceramic reinforcements, such as silicon carbide (SiC), aluminium oxide (Al_2O_3), and zirconium dioxide (ZrO_2). ZrO_2 comes out as a promising reinforcement material because of its high hardness, excellent thermal stability, and resistance to crack propagation. The reinforcement of ZrO_2 to the Al matrix can significantly enhance the composite's load-bearing capacity, increase the wear resistance with a comparable coefficient of friction, making them useful for high-stress tribological applications [9-12].

Despite the various research on Al/ZrO_2 composites, there remain challenges in achieving homogeneous particle dispersion, optimizing interfacial bonding, and understanding the influence of ZrO_2 content on the overall mechanical and tribological characteristics of the composite. The present work aims to systematically investigate the mechanical and tribological properties of Al alloys and Al/ZrO_2 ex-situ composites with varying ZrO_2 content.

The novelty of this research lies in its comprehensive approach to understanding how ZrO_2 content and microstructural characteristics collectively influence the mechanical strength, wear resistance, and surface morphology of Al-based composites. The incorporation of AFM-based surface topography, along with multi-scale property correlations, provides a novel and holistic perspective that contributes to the design of optimized tribo-mechanical materials for engineering applications.

2. Materials and Methodology

To synthesize composites, Al 6061 alloy (elemental composition is given in Table 1) was procured from India Mart, and zirconia powder having an average particle size of 90 nm was procured from Sigma Aldrich (purity ≥99.95).

To fabricate composites ex-situ, the Stir casting route was followed, where PID control electric resistance furnace was utilized for melting. Initially, the furnace temperature was set to 6900 °C with a heating rate of 40 °C/ min. The small pieces of Al kept in a graphite crucible were placed in the furnace. Once the temperature reached the set temperature, hold till the alloy was in molten conditions. Once the alloy is in molten condition, the preheated (at 120^0C for 1 hour) zirconia (ZrO_2) wrapped in aluminium foil was placed in a crucible. After placing the powder, continuous stirring using a stainless steel stirrer was performed for 10 minutes at 150 rpm for homogeneous mixing of the powder in the molten alloy. Before pouring in preheated (200^0C for 90 min) Mold, the hexa-chloro-ethane was used as a degasser to remove entrapped gases from the melts. Four composites were fabricated with varying weight percent (wt. %) of ZrO_2 (with 0, 1, 3, and 5 wt.% of ZrO_2). Further, Table 2 presents the nomenclature of various compositions for easy representation.

Table 1. Elemental composition of Al 6061 alloy [13]

S. No	Element	Weight %
1	Si	0.4-0.8
2	Fe	Maximum- 0.7
3	Cu	0.15-0.4
4	Mg	0.8-1.2
5	Zn	Maximum- 0.25
6	Cr	0.04-0.35
7	Mn	Maximum- 0.15
8	Ti	Maximum- 0.15
9	Other,	Maximum- 0.25
10	total	Balance

Table 2. Nomenclature of alloy and composites

Sr.	Composition	Nomenclature
1	Al 6061 alloy with 0 wt.% ZrO_2	S1
2	Al 6061 alloy with 1 wt.% ZrO_2	S2
3	Al 6061 alloy with 3 wt.% ZrO_2	S3
4	Al 6061 alloy with 5 wt.% ZrO_2	S4

Malvern Panalytical'sX- ray diffractometer (XRD) was used to identify the peaks present in order to confirm the presence of ZrO_2 phase. The Lietz optical microscope was employed to study the optical microstructure (OM) of alloys and composites. Further Nova nano Scanning electron microscopy (SEM) was used to see the distribution, size, and shape of reinforced particles in the matrix.

To investigate the mechanical properties hardness and tensile test was conducted using

Vicker hardness testing setup and an ultimate tensile machine.

A tribological test was conducted using pin on disc tribometer tester. The test was performed for varying loads (10N, 20N, and 30N) and sliding velocity (1 m/sec, 2 m/sec, and 3 m/sec) for a constant sliding distance of 5000m.

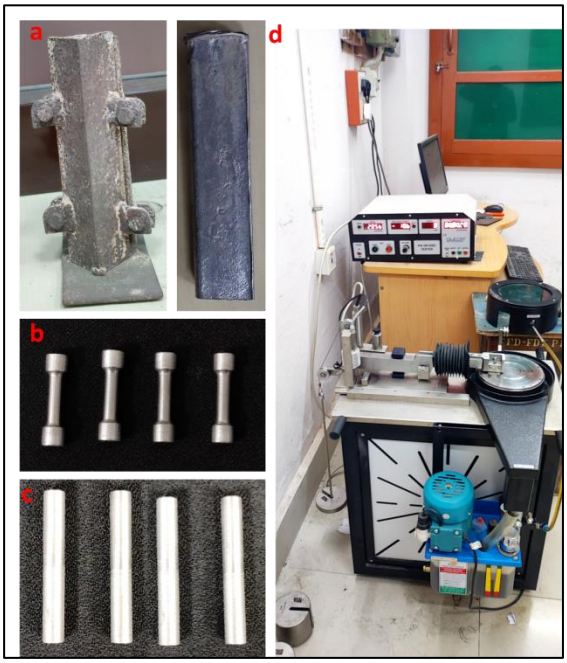

Fig. 1. (a) Mold and ascast sample, (b) Tensile samples, (c) Pin sample for wear and friction test, (d) Pin-on- disc tribometer

3. Results and Discussion

3.1. Characterization (XRD, OM, and SEM) of Alloy and Composites

Figure 2 shows the XRD pattern of the alloy and the composites. Peaks of Al are evident from Fig 2(a) while in Figs. 2(b-c), along with peaks of Al, ZrO2 peaks are also visible, and intensity increases with increasing ZrO2 content, which confirms the presence of reinforced particles in the alloy.

Further microstructure study was conducted using an optical microscope and is given in Fig. 3, which shows the presence of Al rich phase in Fig. 3(a), while in Fig. 3(b), along with Al rich phase, some whitely distributed reinforced particles are visible. Further, it can be observed that with the addition of 3 wt. % of ZrO2 results in grain refinement of the matrix phase, which can further result in an increase in the mechanical properties of composites [14].

A scanning electron microscopy (SEM) image of samples S1 and S4 is presented in Fig. 4, which confirms the presence and distribution of ZrO2 particles (Fig. 4(b)). This is also visible from Fig. 4 that reinforced particles are homogeneously distributed. Some porosity is also visible, which may be due to the presence of second-phase particles and high stirring speed and time for better mixing, which causes entrapment of atmospheric air during casting [15-16].

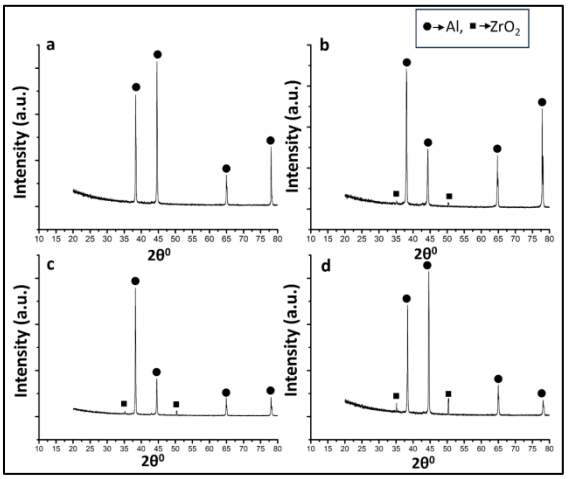

Fig. 2. XRDof samples (a) S1, (b) S2, (c) S3, (d) S4

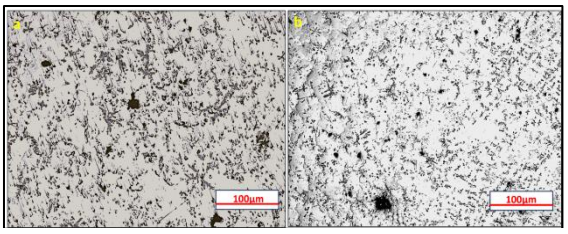

Fig. 3. OM of samples (a) S1, (b) S4

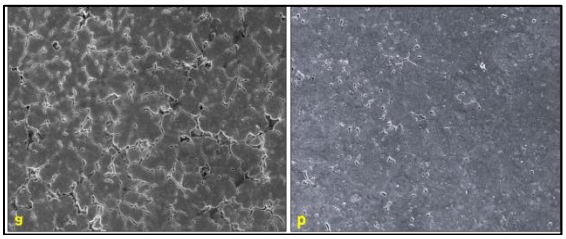

Fig. 4. SEM image of S1 and S4 samples

3.2. Mechanical (Hardness and Tensile) Behaviour of Alloy and Composites

Figure 5 presents the mechanical (hardness and tensile strength) properties of the alloy and composites. It has been observed that with the addition of ZrO_2 particles, there is a significant improvement in the hardness of composites, and it is maximum for sample S4, having a ZrO_2 content of 3 wt. %. This rise in hardness may be due to the presence of hard ZrO_2 particles, as these hard particles act as obstacles to dislocation movement. Also, during mechanical deformation, applied stress is partially transferred from the softer matrix to the harder ZrO_2 particles [17-18]. This results in improved resistance to deformation. Further, dislocations bow around the ZrO_2 particles, creating

additional dislocation density, which contributes to strain hardening and, hence, increased hardness. Further grain refinements also result in an increase in hardness and strength. ZrO_2 particles also participate in the precipitation strengthening mechanism. The presence of ZrO_2 particles facilitates the formation of a finer dispersion of precipitates within the matrix, further enhancing the hardness [19-20].

Figure 5 also presents the tensile strength of the alloy and composites. The addition of ZrO_2 up to 2 wt.% leads to a significant improvement in tensile strength due tothe hardness mechanism. The hard ZrO_2 particles provide an effective load transfer mechanism that enhances the tensile strength of the composite. The addition of ZrO_2 leads to an increase in dislocation density, which contributes to work hardening and improved tensile strength. However, from the Fig 5, it is also visible that beyond 3 wt.%, the addition of ZrO_2 particles can lead to a slight decrease in tensile strength. This slight decrease in tensile strength may be due to the higher concentrations; ZrO_2 particles may have agglomerated, which creates weak points within the matrix. These clusters act as stress concentrators, reducing overall strength. The interfacial bonding between the ZrO_2 particles and the Al matrix may not be as effective at higher concentrations. Poor bonding can lead to debonding during tensile loading, resulting in a reduction of tensile strength [21-23].

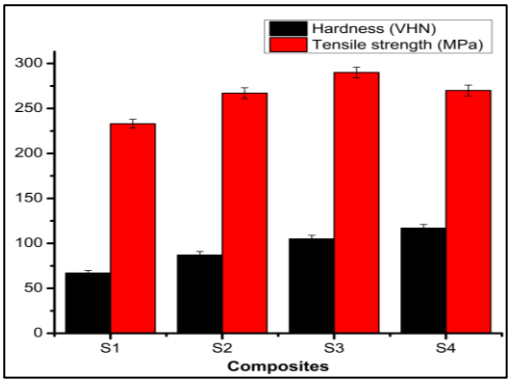

Fig. 5. Mechanical properties (a) Hardness, (b) Tensile strength of alloy and composite

3.3. Wear and Frictional Behaviour of Alloy and Composites

Figures 6-8 present the wear and frictional behaviour of alloys and composites with varying load, sliding velocity, and composition. Fig. 6 presents the wear and coefficient of friction (COF) of samples S1, S2, S3, and S4 at applied loads of 10N, 20 N, and 30 N at constant sliding velocity and distance of 2 m/sec and 5000 m, respectively.

The wear behaviour of Al-based composites reinforced with varying weight percentages of ZrO_2 (1 wt%, 2 wt%, and 3 wt%) demonstrates notable trends in wear resistance and COF under different loading conditions. For samples S2 and S3, there is a linear decrease in wear rates. This reduction is attributed to the reinforcing effect of ZrO_2 particles, which enhances the hardness and wear resistance of the Al matrix. The presence of hard ZrO_2 particles serves as an effective barrier to abrasive wear, reducing the material removal during contact with a counter face. The composites' improved mechanical properties due to ZrO_2 reinforcement led to better performance in wear tests under both 10 N and 20 N loads, reflecting their enhanced ability to withstand mechanical wear [24].

However, for sample S4, the wear does not continue to decrease linearly. Instead, there is a notable plateau in the wear resistance, indicating a diminishing return on wear performance at higher particle concentrations. The rate of decrease in wear becomes less pronounced at this loading, suggesting that excessive ZrO_2 may lead to the agglomeration of particles, which can negatively affect the load-bearing capacity of the composite. Additionally, the increased volume fraction of hard ZrO_2 can introduce internal stress concentrations and potential weak points, which may compromise wear resistance under higher loads, particularly evident at 30 N, where an increase in wear is observed for the 3 wt% ZrO_2 composite [25].

The COF trends similarly to the wear, increasing with both ZrO_2 content and applied load. As the ZrO_2 content rises, the surface of the composite becomes more abrasive, leading to higher friction against the counter face. This behaviour is particularly pronounced at higher loads, where the increased contact pressure enhances the abrasive interactions between the ZrO_2 particles and the counterface material. The combined effect of increased load and ZrO_2 content results in a higher COF, which may contribute to elevated wear rates, especially observed at the 30 N load for the S4 sample.

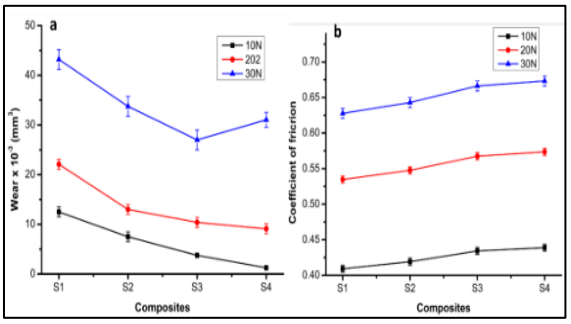

Fig. 6. (a) Wear (mm3) and (b) COF of alloy and composites at sliding velocity of 2 m/sec and sliding distance of 5000 m at varying applied load.

Figure 7 shows the wear and COF behaviour of samples S1, S2, S3, and S4 at constant applied load and sliding distance of 30N and 5000m, respectively, with varying sliding velocity of 1 m/sec, 2 m/sec, and 3m/sec. The wear response of Al-ZrO_2 composites reveals the effects of varying ZrO_2 concentrations (1 wt.%, 2 wt.%, and 3 wt.%) and sliding velocities (1 m/sec, 2 m/sec, and 3 m/sec) under constant applied load. Initially, the reinforcement of ZrO_2 particles at 1 wt.% and 2 wt.% results in a linear decrease in wear, indicating improved wear resistance due to the reinforcement effect of the hard ZrO_2 particles. This rise may be due to enhanced hardness, load transfer, and effective dislocation pinning, which combinedly contribute to the composite's property to withstand wear. However, at 3 wt.% ZrO_2, the rate of wear reduction becomes less significant, suggesting that excessive particle concentration may result in agglomerations and potential weak points within the composite structure.

When the sliding velocity is increased, the wear behaviour changes significantly. At sliding velocities of 1 m/sec and 2 m/sec, wear rates increase for all compositions, indicating that higher velocities exacerbate wear, potentially due to increased frictional heat and abrasive interactions between the composite and the counter face. This rise in wear at lower velocities highlights the importance of dynamic conditions on wear behaviour. Interestingly, at a sliding velocity of 3 m/sec, wear is slightly lower than at 2 m/secfor all the samples. This counterintuitive result may be due to the formation of a lubricating layer or a transient wear regime that develops at higher velocities, reducing direct contact and subsequent wear.

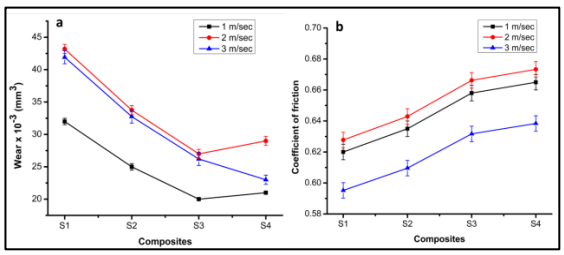

Fig. 7. (a) Wear (mm^3) and (b) COF of alloy and composites at applied load of 30N and sliding distance of 5000 m at varying sliding velocity

Furthermore, COFfollows a consistent trend with rising ZrO_2 amount and sliding velocity. As the amount of ZrO_2 increases, the COFrises, reflecting the abrasive nature of the ZrO_2 particles. However, at the highest sliding velocity of 3 m/sec, COF is the lowest for all samples. This suggests that the wear mechanisms may shift at higher velocities, potentially due to the reduction of direct particle-to-surface contact and the establishment of a more stable tribological regime that minimises frictional resistance.

Figure 8 depicts the wear and COF behaviour of samples S1, S2, S3, and S4 at constant applied load, sliding velocity, and sliding distance of 30 N, 3m/sec, and 5000m, respectively. The reinforcement of ZrO_2 particles to Al alloys affects their wear behaviour and COF under given conditions, such as a constant load of 30 N, a sliding velocity of 3 m/sec, and a sliding distance of 5000 m. At lower amounts of reinforced particles (1 wt.% and 2 wt.%), ZrO_2 increases the hardness and tensile strength of the matrix, lowering wear throughdecreasing material removal during sliding. The ZrO_2 particles cause better load dispersion, reducing localized wear and the formation of a protective transfer layer, which further reduces wear by decreasing direct contact between sliding surfaces.

Further, the reinforcement of ZrO_2 particles results inrise in the COFbecause of its abrasive nature, leading to more surface roughness and interfacial resistance. At 3 m/sec, the COF rises owing to the more kinetic energy and increased abrasive interactions between ZrO_2 and the counter body. Despite the decrease in wear, the increased COF highlights a complex interplay of adhesion, abrasion, and surface interactions, emphasizing the need to balance ZrO_2 content for optimal wear performance and COF in composites.

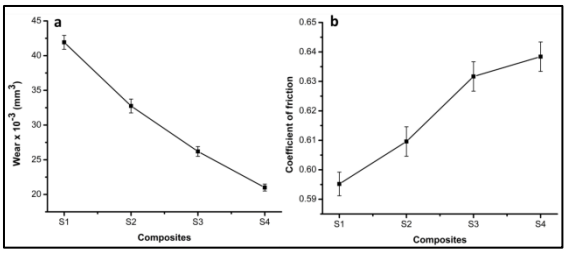

Fig. 8. (a) Wear (mm^3) and (b) COF of alloy and composites at constant applied load, sliding distance, and sliding velocity of 30 N, 3 m/sec, and 5000 m with varying composition.

3.4 Topographical Behaviour of Alloy and Composites

Figure 9 illustrates the scanning electron microscopy (SEM) images of the worn surfaces of samples S1, S2, S3, and S4, tested under constant conditions of 30 N load, 3 m/sec sliding velocity, and a sliding distance of 5000 m. As seen in Fig. 9(a) for sample S1, the wear mechanisms include ploughing, delamination, and the formation of wear grooves, indicating significant material loss and consequently high wear rates. This suggests that the absence of hard reinforcements in sample S1 leads to a rough surface that is more susceptible to abrasive wear.

In contrast, the addition of hard ZrO_2 particles in samples S2 and S3 results in a smoother topography. The wear observed in these samples is characterized primarily by wear grooves, indicating a transition to more favourable wear behaviour and high wear resistance. This shift suggests that the ZrO_2 particles effectively mitigate the wear process by enhancing the surface hardness and providing a barrier against material loss. The findings from the SEM analysis are consistent with those observed in Figures 6-8, supporting the conclusion that ZrO_2 reinforcement significantly improves wear performance.

Furthermore, atomic force microscopy (AFM) analysis, as shown in Fig. 10, further corroborates these observations. The AFM results reveal that sample S1 exhibits the highest average surface roughness, indicating a rougher surface associated with greater material loss and higher wear rates. In contrast, samples S2 and S3 demonstrate decreased average surface roughness values, reinforcing the notion of lower wear due to the effective reinforcement provided by ZrO_2 particles [26-28].

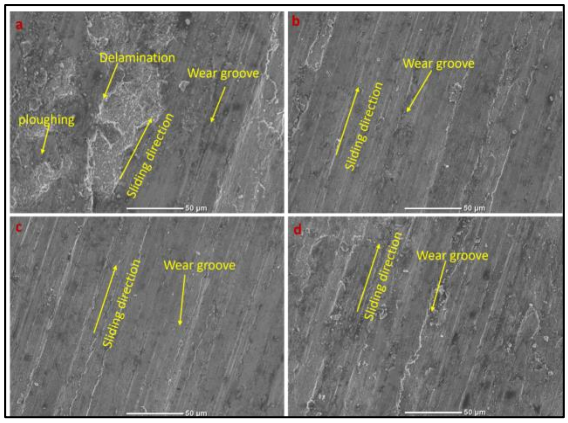

Fig. 9. SEM of worn surface of samples (a) S1, (b) S2, (c) S3, (d) S4 at Constant applied load, sliding distance, and sliding velocity of 30 N, 3m/sec, and 5000 m respectively.

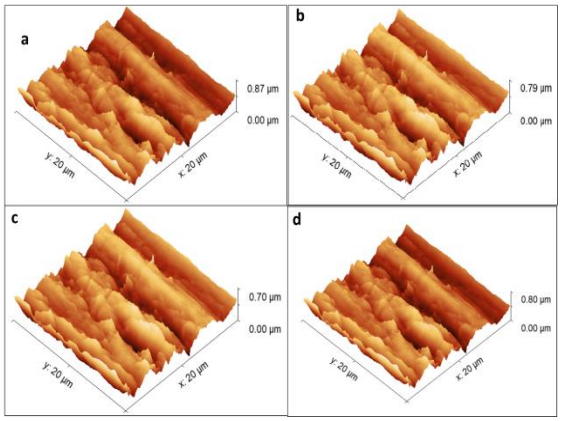

Fig. 10. AFM of worn surface of samples (a) S1, (b) S2, (c) S3, (d) S4 at constant applied load, sliding distance, and sliding velocity of 30 N, 3 m/sec, and 5000 m, respectively.

4. Conclusions

1. Adding ZrO_2 particles to Al alloys enhances Vickers hardness and significantly improves tensile strength up to 3 wt.%. However, at 5 wt.%, particle clustering and bonding issues reduce tensile strength. Understanding these effects is essential for optimizing the mechanical properties of Al-ZrO_2 composites.
2. ZrO_2 enhances wear resistance at 1 wt.% and 2wt.%, but shows decreased performance at 3 wt.% under certain loads. The rising coefficient of friction with increased ZrO_2 content and load highlights the need for optimizing particle reinforcement in Al composites for better tribological performance.
3. ZrO_2 improves wear resistance at lower concentrations, but wear performance varies with sliding velocity, showing increased rates at lower speeds and reduced wear at 3 m/s, while the coefficient of friction increases with ZrO_2 content and velocity, highlighting the need for optimization in Al-ZrO_2 composites.
4. Adding ZrO_2 to Al alloys reduces wear rates at 30 N and 3 m/sec, but increases the coefficient of friction due to the particles' abrasiveness and interfacial interactions, highlighting the need for balanced optimization of ZrO_2 content in composites.
5. The addition of ZrO_2 particles to Al alloys leads to a decrease in average surface roughness value from 0.87µm to 0.70µm and reduced wear rates, confirming their effectiveness in enhancing wear resistance.

Funding Statement

This research did not receive any specific grant from funding agencies in the public, commercial, or not-for-profit sectors.

Conflicts of Interest

The author declares that there is no conflict of interest regarding the publication of this article.

References

[1] Huang, Q., Shi, X., Xue, Y., Zhang, K. & Wu, C., 2023. Recent progress on surface texturing and solid lubricants in tribology: Designs, properties, and mechanisms. *Materials Today Communications*, 35, p.105854. ISSN

2352-4928, doi.org/10.1016/j.mtcomm.2023.105854.

[2] Kumar, V., Gautam, G., Mohan, A. and Mohan, S., 2023. Tribology of in-situ Zn-Al/ZrB2 composites in reciprocating motion. *Intermetalcast*, 17, pp. 182–194. doi: 10.1007/s40962-022-00764-2.

[3] Gupta, M., Gangil, B. and Ranakoti, L., 2020. Mechanical and tribological characterizations of Al/TiB2 composites. *International Engineering Journal*, 13, 10.26488/IEJ.13.4.1250.

[4] Liang, Y., Wang, W., Zhang, Z., Xing, H., Wang, C., Zhang, Z., Guan, T. and Gao, D., 2023. Effect of material selection and surface texture on tribological properties of key friction pairs in water hydraulic axial piston pumps: A review. *Lubricants*, 11(8), p.324. doi.org/10.3390/lubricants11080324.

[5] Ranakoti, L., Gangil, B., Rajesh, P., Singh, T., Sharma, S., Li, C., Ilyas, R.A. and Mahmoud, O., 2022. Effect of surface treatment and fiber loading on the physical, mechanical, sliding wear, and morphological characteristics of tasar silk fiber waste-epoxy composites for multifaceted biomedical and engineering applications: Fabrication and characterizations. *Journal of Materials Research and Technology*, 19, 10.1016/j.jmrt.2022.06.024.

[6] Maurya, R., Kumar, V., Gautam, S. et al., 2024. Investigation of microstructural and mechanical characteristics of Al-ZrO2 composites fabricated by stir casting. *Interactions*, 245, p. 301. doi.org/10.1007/s10751-024-02163-x

[7] Kumar, V., Mishra, A., Mohan, S. and Mohan, A., 2021. Utilization of waste graphite crucible for the fabrication of ex-situ AA1100/Graphite composite via stir casting route. *Materials Today: Proceedings*, 46 (Part 3), pp. 1481–1486. doi.org/10.1016/j.matpr.2020.11.353.

[8] Das, S., 2004. Development of aluminium alloy composites for engineering applications. *Transactions of the Indian Institute of Metals*., 57 pp. 325-334.

[9] Chatterjee, A., Sen, S., Paul, S., Roy, P., Seikh, A.H., Alnaser, I.A., Das, K., Sutradhar, G. & Ghosh, M., 2023. Fabrication and characterization of SiC-reinforced aluminium matrix composite for brake pad applications. *Metals*, 13(3), 584. doi.org/10.3390/met13030584.

[10] Kok, M., 2005. Production and mechanical properties of Al_2O_3 particle-reinforced 2024 aluminium alloy composites. *Journal of Materials Processing Technology*, 161(3), pp. 381–387. doi.org/10.1016/j.jmatprotec.2004.07.068.

[11] Younes, R., Amokrane, B., Sadeddine, A., Mouadji, Y., Bilek, A. & Benabbas, A., 2016. Effect of TiO_2 and ZrO_2 reinforcements on properties of Al_2O_3 coatings fabricated by thermal flame spraying. *Transactions of Nonferrous Metals Society of China*, 26, pp. 1345–1352. 10.1016/S10036326(16)64237-1.

[12] Yadav, A., Gautam, G. & Mohan, S., 2023. Microstructure–mechanical property correlation in cooling slope cast Al–Si/Mg_2Si–x wt.% TiB_2 (x = 0, 1, 3 and 5) in-situ hybrid composites. *Silicon*, 15, pp. 1–10. 10.1007/s12633-023-02587-0.

[13] ASM International, 1990. Metals handbook. Vol. 2, *Properties and selection – nonferrous alloys and special-purpose materials*. 10th ed. Materials Park, OH, ASM International.

[14] Kumar, V., Kushwaha, S., Ankit, Sharma, A. & Gautam, G., 2024. Microstructural and mechanical analysis of heat-treated Zn–Al alloy and Zn–Al/ZrB_2 composites. *Materials Letters*, 366, 136573. doi.org/10.1016/j.matlet.2024.136573.

[15] Ahmad, S. & Ghazali, M.I., 2005. The effects of porosity on mechanical properties of cast discontinuous reinforced metal–matrix composite. *Journal of Composite Materials*, 39, pp. 451–466. 10.1177/0021998305047096.

[16] Kumar, V., Mishra, A., Mohan, S. & Mohan, A., 2019. Fabrication of stir-cast ZA/ZrB_2 reinforced in-situ composites. *Materials Research Express*, 6(12). DOI 10.1088/2053-1591/ab53f2.

[17] Sansoz, F. & Stevenson, K., 2011. Relationship between hardness and dislocation processes in a nanocrystalline metal at the atomic scale. *Physical Review B: Condensed Matter*, 83, 224101. 10.1103/PhysRevB.83.224101.

[18] *Kumar*, V., Gautam, G., Yadav, A.K., Mohan, A. & Mohan, S., 2023. Influence of in-situ formed ZrB_2 particles on dry sliding behavior of ZA based metal matrix composites. *Inter Metalcast*, 17, pp. 786–800. doi.org/10.1007/s40962-022-00806-9.

[19] Gutierrez-Urrutia, I., Muñoz-Morris, M.A. & Morris, D., 2005. The effect of coarse second-phase particles and fine precipitates

on microstructure refinement and mechanical properties of severely deformed Al alloy. *Materials Science and Engineering A,* 394, pp. 399–410. 10.1016/j.msea.2004.11.025.

[20] Zhan, L., Lin, J. & Balint, D., 2012. Microstructure control in creep–age forming of aluminium panels. In: J. Lin, D. Balint & M. Pietrzyk, eds. *Microstructure evolution in metal forming processes*. *Cambridge: Woodhead Publishing*, pp. 298–336. doi.org/10.1533/9780857096340.3.298.

[21] Kumar, V., Gautam, G., Singh, A., Singh, V., Mohan, S. & Mohan, A., 2022. Tribological behaviour of ZA/ZrB_2 in situ composites using response surface methodology and artificial neural network. *Surface Topography: Metrology and Properties*, 10(4). 10.1088/2051-672X/ac9426.

[22] Singh, T., Singh, V., Ranakoti, L. & Kumar, S., 2023 Optimization on tribological properties of natural fiber reinforced brake friction composite materials: Effect of objective and subjective weighting methods. *Polymer Testing*, 117, 107873. doi.org/10.1016/j.polymertesting.2022.107873.

[23] Yadav, A.K., Kumar, V., Ankit & Mohan, S., 2023. Microstructure and mechanical properties of an in situ Al 356–Mg_2Si–TiB_2 hybrid composite prepared by stir and cooling slope casting. *Inter Metalcast*, 17, pp. 740–752. doi.org/10.1007/s40962-022-00804-x.

[24] Ankit, Kumar, V., Gautam, G., Yadav, A.K., Singh, K.K. & Mohan, S., 2023. Prediction of tribological performance of Cu–Gr–TiC composites based on response surface methodology and worn surface analysis. *Physica Scripta*. doi.10.1088/1402-4896/acff8d

[25] Basu, B., Vleugels, J. & Van Der Biest, O., 2004. ZrO_2–Al_2O_3 composites with tailored toughness. *Journal of Alloys and Compounds*, 372(1–2), pp. 278–284. 10.1016/j.jallcom.2003.09.157.

[26] Kumar, V., Ranakoti, L., Gautam, G., Negi, A. & Singh, T., 2024. Erosive wear and topographical study of zinc-aluminum based composite reinforced with in-situ formed ZrB_2 particles. *Results in Engineering*, 22, 102346. doi.org/10.1016/j.rineng.2024.102346.

[27] Szeri, A.Z., 2003. *Tribology*. In: R.A. Meyers, ed. *Encyclopedia of Physical Science and Technology*. 3rd ed. San Diego: Academic Press, pp. 127–152. doi.org/10.1016/B0-12-227410-5/00791-2.

[28] Kumar, V., Gautam, G., Ankit, Mohan, A. & Mohan, S., 2023. Correlating surface topography of relaxed layer of ZA/ZrB_2 in situ composites to wear and friction. *Surface Topography: Metrology and Properties*, 11(2). DOI 10.1088/2051-672X/acc881.

[29] Esfe, M.H., Alidoust, S., Hosseini Tamrabad, S.N., Toghraie, D. & Hatami, H., 2023. Thermal conductivity of MWCNT–TiO_2/Water–EG hybrid nanofluids: Calculating the price performance factor (PPF) using statistical and experimental methods (RSM). *Case Studies in Thermal Engineering*, 48, 103094. doi.org/10.1016/j.csite.2023.103094

[30] Hatami, H., Tavallaei, R., Karajabad, M. & Toghraie, D., 2023. Development of knowledge management in investigating the rheological behavior of SiO_2/SAE50 nano-lubricant by response surface methodology (RSM). *Tribology International*, 187(4), 108667. doi.org/10.1016/j.triboint.2023.108667

[31] Hatami, H., Fathollahi, A., 2018. Theoretical and Numerical Study and Comparison of the Inertia Effects on the Collapse Behavior of Expanded metal tube Absorber with Single and Double Cell under Impact Loading. *Amirkabir Journal of Mechanical Engineering*, 50(5), pp. 999-1014. doi: 10.22060/MEJ.2017.12016.5242

[32] Mousavizadeh, S. A., Hosseini, M., hatami, H., 2021. Experimental Studies on Energy Absorption of Curved Steel Sheets under Impact Loading and the Effect of Pendentive on the Deformation of Samples. *Journal of Modeling in Engineering*, 18(63), pp. 27-40. Doi.10.22075/JME.2020.18501.1765